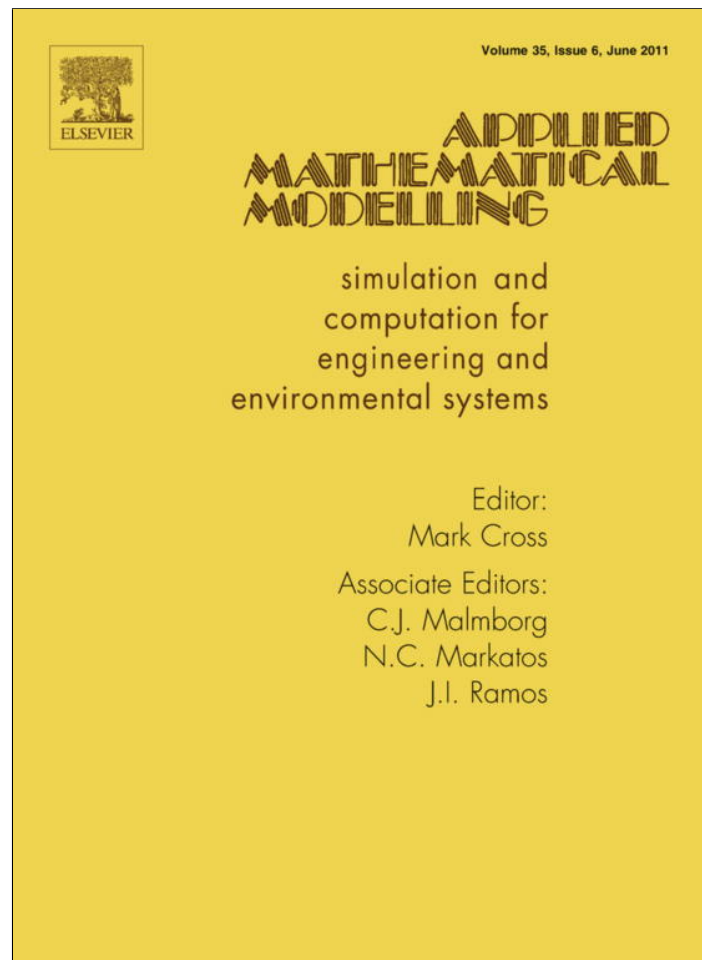


Provided for non-commercial research and education use.  
Not for reproduction, distribution or commercial use.



This article appeared in a journal published by Elsevier. The attached copy is furnished to the author for internal non-commercial research and education use, including for instruction at the authors institution and sharing with colleagues.

Other uses, including reproduction and distribution, or selling or licensing copies, or posting to personal, institutional or third party websites are prohibited.

In most cases authors are permitted to post their version of the article (e.g. in Word or Tex form) to their personal website or institutional repository. Authors requiring further information regarding Elsevier's archiving and manuscript policies are encouraged to visit:

<http://www.elsevier.com/copyright>



Contents lists available at ScienceDirect

## Applied Mathematical Modelling

journal homepage: [www.elsevier.com/locate/apm](http://www.elsevier.com/locate/apm)

# Inverse prediction of frictional heat flux and temperature in sliding contact with a protective strip by iterative regularization method

Wen-Lih Chen, Yu-Ching Yang\*

Clean Energy Center, Department of Mechanical Engineering, Kun Shan University, Yung-Kang City, Tainan 710-03, Taiwan, ROC

## ARTICLE INFO

## Article history:

Received 6 June 2010

Received in revised form 25 November 2010

Accepted 30 November 2010

Available online 15 December 2010

## Keywords:

Inverse problem

Sliding-contact process

Heat generation

Conjugate gradient method

## ABSTRACT

In this study, an inverse algorithm based on the conjugate gradient method and the discrepancy principle is applied to estimate the unknown time-dependent frictional heat flux at the interface of two semi-spaces, one of them is covered by a strip of coating, during a sliding-contact process from the knowledge of temperature measurements taken within one of the semi-space. It is assumed that no prior information is available on the functional form of the unknown heat generation; hence the procedure is classified as the function estimation in inverse calculation. Results show that the relative position between the measured and the estimated quantities is of crucial importance to the accuracy of the inverse algorithm. The current methodology can be applied to the prediction of heat generation in engineering problems involving sliding-contact elements.

© 2010 Elsevier Inc. All rights reserved.

## 1. Introduction

The knowledge of the flash temperatures at a sliding interface is of fundamental importance for the tribological behavior of materials and has immediate application in the fields of lubrication, metal cutting, grinding and forming tools, mechanical seals, electric contacts, etc. The determination of the flash temperatures requires the knowledge of frictional heat generated on the sliding-contact interface. When two objects come into a sliding contact, nearly all the energy dissipated by friction is converted into heat, which is distributed between the two objects, influences friction and wear characteristics, and appreciably raises the temperature at the adjacent area of the sliding interface. Theoretically, the frictional heat is considered broadly as a function of sliding velocity, friction coefficient, and contact pressure. However, the establishment of the frictional heat has never been an easy task. In the past, there have been many investigations focusing on the flash temperature of a sliding contact [1–4]. However, for the result to be realistic, appropriate solutions are needed for geometric configuration and sliding criteria. The problem of sliding contact is of significant importance in yet another engineering application. In order to obtain specific technical, protecting, or decorative properties of an object, it is a common practice nowadays to deposit a thin layer of alien material, called coating, on friction elements' surface. The wear and contact characteristics of the friction couples can be largely improved by applying protective sprayed coatings and films, in particular, made of composite materials. The technological development today makes it possible to make single- or multi-layer coatings of thickness varying in the range of micrometers and millimeters. As a result, better usable properties than the surface of foundation can be achieved. Among these properties, tribological and thermal properties of both coating and foundation affect the heat generation inside them and wear intensity on the area of rubbing. Therefore, there is a need to conduct thermal analysis on these issues, especially those associated with friction processes in various machine elements on which thin coatings with alien materials are deposited, for scientific and technical purposes [5–7].

\* Corresponding author.

E-mail address: [ycyang@mail.ksu.edu.tw](mailto:ycyang@mail.ksu.edu.tw) (Y.-C. Yang).

**Nomenclature**

$d$	thickness of the strip (m)
$J$	functional
$J'$	gradient of functional
$k$	thermal conductivity ( $\text{W m}^{-1} \text{K}^{-1}$ )
$P$	compressive pressure ( $\text{N m}^{-2}$ )
$p$	direction of descent
$q$	intensity of the frictional heat flux ( $\text{W m}^{-2}$ )
$T$	temperature (K)
$T_0$	initial temperature of the system (K)
$t$	time coordinate (s)
$V$	sliding velocity ( $\text{m s}^{-1}$ )
$Y$	measured temperature (K)
$z$	spatial coordinate (m)

*Greek symbols*

$\Delta$	small variation quality
$\alpha$	thermal diffusivity ( $\text{m}^2 \text{s}^{-1}$ )
$\beta$	step size
$\gamma$	conjugate coefficient
$\eta$	very small value
$\lambda$	variable used in adjoint problem
$\sigma$	standard deviation
$\tau$	transformed time coordinate
$\varpi$	random variable

*Superscripts/subscripts*

$K$	iterative number
$m$	measurement position
*	dimensionless quantity

Inverse analysis becomes a valuable alternative when the direct measurement of data is difficult or the measuring process is very expensive, for example, the determination of heat transfer coefficients, the detection of contact resistance, the estimation of unknown thermophysical properties of new materials, the prediction of damage in the structure fields, the detection of fouling-layer profiles on the inner wall of a piping system, the optimization of geometry, the prediction of crevice and pitting in furnace wall, the determination of heat flux at the outer surface of a vehicle re-entry, earthquake study [8], and so on. Over the past decades, the studies of inverse heat conduction problem (IHCP) have offered convenient alternatives, which largely scale down experimental work, to obtain accurate thermophysical quantities in many heat conduction problems. To date, a variety of analytical and numerical techniques have been developed for the solution of IHCP, for example, the conjugate gradient method (CGM) [9–14], the function-specification method [15], the space-marching method [16], the Tikhonov regularization method [17], and the genetic algorithm [18].

The estimation of heat source strength has been the main theme of a number of studies. For example, Neto Silva and Ozisik [19] applied the conjugate gradient method to estimate the timewise varying strength of a line heat source placed at a specified location in a rectangular region with insulated boundaries. Yang [20] used the finite-difference method in conjunction with the linear least-squares scheme to estimate the strength of the temporal dependent heat source in an infinitely long bar. Niliot and Lefevre [21] adopted a parameter estimation approach based on the boundary element method to solve the inverse problem for point heat source identification. Jin and Marin [22] presented the use of the method of fundamental solutions (MFS) for recovering the heat source in steady-state heat conduction problems from boundary temperature and heat flux measurements. Lee et al. [23] applied the conjugate gradient method to estimate the unknown space- and time-dependent heat source in aluminum-coated tapered optical fibers for scanning near-field optical microscopy, by reading the transient temperature data at the measurement positions. Recently, Chen et al. [24] estimated the heat generation at the interface of cylindrical bars during friction process by using the conjugate gradient method.

The main objective of the present study is to develop an inverse analysis to estimate the frictional heat generation at the interface of two semi-spaces, where one of them is homogeneous and the other is a semi-infinite foundation with surface covered by a thin layer of coating, during transient frictional heating. An analysis of this kind poses significant implications on the study of the problems associated with sliding-contact interface mentioned earlier. However, it is well known that inverse problems are in general unstable in the sense that small measurement errors in the experimental data may amplify significantly the errors in their solutions. As a consequence, the inverse problems are ill-posed and hence they are more difficult to solve than the direct problems. In some even worse scenarios, an inverse analysis could fail if the functional rela-

relationship between the measured quantity and the estimated quantity is too weak. Such weak relationship exists in many engineering problems, for example, convective heat transfer and transient heat conduction. Chen and Yang [13] reported that the relative position between the measured and estimated quantities is one of the most crucial factors to whether an inverse analysis being successful or not in a heat convection problem. Detailed discussion on the mechanism behind the phenomenon was also documented. On the other hand, many studies [25–27] have also documented the sensitive nature of the predictive accuracy of an inverse solution on the relative position between the measured and estimated quantities in transient heat conduction problems. However, most of them tackled the issue by just reporting the finding, and there has not been a study probing deeper to reveal the mechanism behind the sensitivity. Therefore, a part of this paper is devoted to shed more light into the mechanism responsible for the sensitivity of the solution accuracy.

In this study, we present the conjugate gradient method and the discrepancy principle [28] to estimate the time-varying frictional heat generation by using the simulated temperature measurements. Subsequently, the distributions of temperature in the semi-spaces and coating can be determined as well. The conjugate gradient method with an adjoint equation, also called Alifanov's iterative regularization method, belongs to a class of iterative regularization techniques, which mean the regularization procedure is performed during the iterative processes, thus the determination of optimal regularization conditions is not needed. In this approach, a sensitivity problem is solved to determine the step size in the direction of descent, and an adjoint problem is solved to determine the gradient of the functional. No prior information is used in the functional form of the heat generation variation with time. On the other hand, the discrepancy principle is used to terminate the iteration process in the conjugate gradient method.

## 2. Analysis

### 2.1. Direct problem

To illustrate the methodology for developing expressions for the use in determining the unknown time-dependent heat generation during transient frictional heating at the interface of two semi-spaces, where one of them is homogeneous and the other is a semi-infinite foundation with surface covered by a strip of coating. Since the thickness of a coating is very small compared with the widths and breadths of a coated surface and the friction element that makes contact with the coated surface, the two spaces can be assumed to be infinite at  $x$ - and  $y$ -directions. Therefore the problem can be simplified as a 1D problem where temperature variation occurs only at the  $z$ -direction. Fig. 1 shows the configuration of this 1D transient heat transfer problem. Here, the perfect heat contact between the strip and the substrate is assumed. It is supposed that the compressive pressures  $P(t)$  are applied to the infinities in semi-spaces. The homogeneous upper semi-space slides with velocity  $V(t)$  in the direction of  $y$ -axis on the coating surface. Then, the dimensionless governing equations and the associated boundary and initial conditions for the system can be written as [7]:

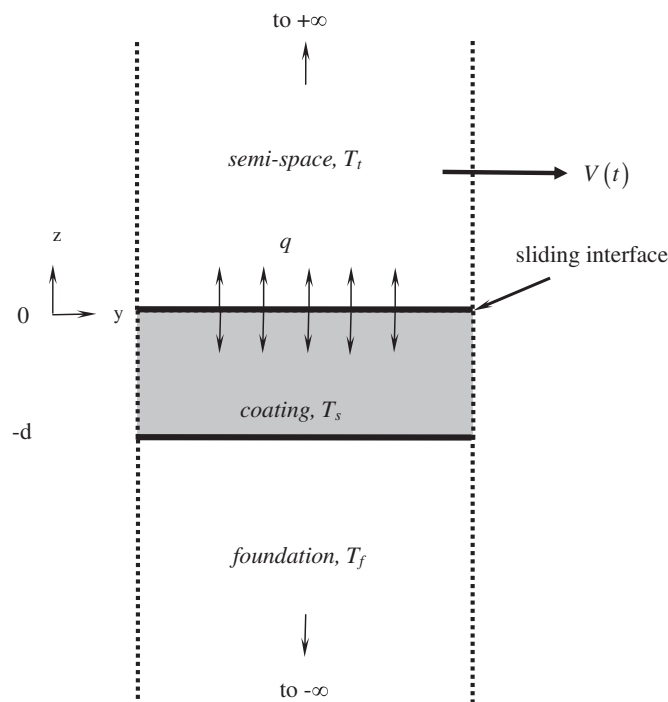


Fig. 1. Geometry and coordinate system.

$$\frac{\partial^2 T_t^*(z^*, t^*)}{\partial z^{*2}} = \frac{1}{\alpha_{ts}} \frac{\partial T_t^*(z^*, t^*)}{\partial t^*}, \quad 0 \leq z^* < \infty, \quad t^* > 0, \quad (1)$$

$$\frac{\partial^2 T_s^*(z^*, t^*)}{\partial z^{*2}} = \frac{\partial T_s^*(z^*, t^*)}{\partial t^*}, \quad -1 \leq z^* \leq 0, \quad t^* > 0, \quad (2)$$

$$\frac{\partial^2 T_f^*(z^*, t^*)}{\partial z^{*2}} = \frac{1}{\alpha_{fs}} \frac{\partial T_f^*(z^*, t^*)}{\partial t^*}, \quad -\infty < z^* \leq -1, \quad t^* > 0, \quad (3)$$

$$T_s^*(0, t^*) = T_t^*(0, t^*), \quad z^* = 0, \quad t^* > 0, \quad (4)$$

$$\frac{\partial T_s^*(0, t^*)}{\partial z^*} - k_{ts} \frac{\partial T_t^*(0, t^*)}{\partial z^*} = q^*(t^*), \quad z^* = 0, \quad t^* > 0, \quad (5)$$

$$T_s^*(-1, t^*) = T_f^*(-1, t^*), \quad z^* = -1, \quad t^* > 0, \quad (6)$$

$$\frac{\partial T_s^*(-1, t^*)}{\partial z^*} = k_{fs} \frac{\partial T_f^*(-1, t^*)}{\partial z^*}, \quad z^* = -1, \quad t^* > 0, \quad (7)$$

$$T_t^*(z^*, t^*) \rightarrow 0, \quad z^* \rightarrow \infty, \quad t^* > 0, \quad (8)$$

$$T_f^*(z^*, t^*) \rightarrow 0, \quad z^* \rightarrow -\infty, \quad t^* > 0, \quad (9)$$

$$T_t^*(z^*, 0) = 0, \quad 0 \leq z^* < \infty, \quad t^* = 0, \quad (10)$$

$$T_s^*(z^*, 0) = 0, \quad -1 \leq z^* \leq 0, \quad t^* = 0, \quad (11)$$

$$T_f^*(z^*, 0) = 0, \quad -\infty < z^* \leq -1, \quad t^* = 0, \quad (12)$$

where the subscripts *t*, *s*, and *f* refer to the regions of top semi-space, strip of coating, and foundation, respectively.  $q^*(t^*)$  in Eq. (5) is the dimensionless frictional heat output. In general, the frictional heat output should be a function of the compressive pressure, friction coefficient, and sliding velocity.

The dimensionless variables used in the above formulation are defined as follows:

$$\begin{aligned} z^* &= z/d, \quad t^* = \alpha_s t/d^2, \quad q^* = dq/k_s T_0, \\ T_t^* &= (T_t - T_0)/T_0, \quad T_s^* = (T_s - T_0)/T_0, \quad T_f^* = (T_f - T_0)/T_0, \\ \alpha_{ts} &= \alpha_t/\alpha_s, \quad \alpha_{fs} = \alpha_f/\alpha_s, \quad k_{ts} = k_t/k_s, \quad k_{fs} = k_f/k_s, \end{aligned} \quad (13)$$

where *d* is the thickness of the coating, *q* is the frictional heat generation, and  $T_0$  is the temperature of the system at  $t = 0$ . *k* and  $\alpha$  are the thermal conductivity and thermal diffusivity, respectively. The direct problem considered here is concerned with the determination of the medium temperature when the frictional heat output  $q^*(t^*)$ , thermophysical properties of the system, and initial and boundary conditions are known.

### 2.2. Inverse problem

For the inverse problem, the function  $q^*(t^*)$  is regarded as being unknown, while everything else in Eqs. (1)–(12) is known. In addition, temperature readings taken at  $z = z_m$  in the strip region are considered available. The objective of the inverse analysis is to predict the unknown time-dependent function of intensity of the frictional heat generation,  $q^*(t^*)$ , merely from the knowledge of these temperature readings. Let the measured temperature at the measurement position  $z = z_m$  and time *t* be denoted by  $Y(z_m, t)$ . Then this inverse problem can be stated as follows: by utilizing the above mentioned measured temperature data  $Y(z_m, t)$ , the unknown  $q^*(t^*)$  is to be estimated over the specified time domain.

The solution of the present inverse problem is to be obtained in such a way that the following functional is minimized:

$$J[q^*(t^*)] = \int_{t^*=0}^{t_f^*} [T_s^*(z_m^*, t^*) - Y^*(z_m^*, t^*)]^2 dt^*, \quad (14)$$

where  $Y^*(z_m^*, t^*) = [Y(z_m, t) - T_0]/T_0$ , and  $Y(z_m, t)$  is the estimated (or computed) temperature at the measurement location  $z = z_m$ . In this study,  $Y^*(z_m^*, t^*)$  are determined from the solution of the direct problem given previously by using an estimated  $q^{*K}(t^*)$  for the exact  $q^*(t^*)$ , here  $q^{*K}(t^*)$  denotes the estimated quantities at the *K*th iteration.  $t_f^*$  is the final time of the measurement. In addition, in order to develop expressions for the determination of the unknown  $q^*(t^*)$ , a “sensitivity problem” and an “adjoint problem” are constructed as described below.

2.3. Sensitivity problem and search step size

The sensitivity problem is obtained from the original direct problem defined by Eqs. (1)–(12) in the following manner: It is assumed that when  $q^*(t^*)$  undergoes a variation  $\Delta q^*(t^*)$ ,  $T_t^*(z^*, t^*)$ ,  $T_s^*(z^*, t^*)$ , and  $T_f^*(z^*, t^*)$  are perturbed by  $T_t^* + \Delta T_t^*$ ,  $T_s^* + \Delta T_s^*$ , and  $T_f^* + \Delta T_f^*$ , respectively. Then replacing in the direct problem  $q^*(t^*)$  by  $q^*(t^*) + \Delta q^*(t^*)$ ,  $T_t^*$  by  $T_t^* + \Delta T_t^*$ ,  $T_s^*$  by  $T_s^* + \Delta T_s^*$ , and  $T_f^*$  by  $T_f^* + \Delta T_f^*$ , subtracting from the resulting expressions the direct problem, and neglecting the second-order terms, the following sensitivity problem for the sensitivity function  $\Delta T_t^*$ ,  $\Delta T_s^*$ , and  $\Delta T_f^*$  can be obtained:

$$\frac{\partial^2 \Delta T_t^*(z^*, t^*)}{\partial z^{*2}} = \frac{1}{\alpha_{ts}} \frac{\partial \Delta T_t^*(z^*, t^*)}{\partial t^*}, \quad 0 \leq z^* < \infty, \quad t^* > 0, \tag{15}$$

$$\frac{\partial^2 \Delta T_s^*(z^*, t^*)}{\partial z^{*2}} = \frac{\partial \Delta T_s^*(z^*, t^*)}{\partial t^*}, \quad -1 \leq z^* \leq 0, \quad t^* > 0, \tag{16}$$

$$\frac{\partial^2 \Delta T_f^*(z^*, t^*)}{\partial z^{*2}} = \frac{1}{\alpha_{fs}} \frac{\partial \Delta T_f^*(z^*, t^*)}{\partial t^*}, \quad -\infty < z^* \leq -1, \quad t^* > 0, \tag{17}$$

$$\Delta T_s^*(0, t^*) = \Delta T_t^*(0, t^*), \quad z^* = 0, \quad t^* > 0, \tag{18}$$

$$\frac{\partial \Delta T_s^*(0, t^*)}{\partial z^*} - k_{ts} \frac{\partial \Delta T_t^*(0, t^*)}{\partial z^*} = \Delta q^*(t^*), \quad z^* = 0, \quad t^* > 0, \tag{19}$$

$$\Delta T_s^*(-1, t^*) = \Delta T_f^*(-1, t^*), \quad z^* = -1, \quad t^* > 0, \tag{20}$$

$$\frac{\partial \Delta T_s^*(-1, t^*)}{\partial z^*} = k_{fs} \frac{\partial \Delta T_f^*(-1, t^*)}{\partial z^*}, \quad z^* = -1, \quad t^* > 0, \tag{21}$$

$$\Delta T_t^*(z^*, t^*) \rightarrow 0, \quad z^* \rightarrow \infty, \quad t^* > 0, \tag{22}$$

$$\Delta T_f^*(z^*, t^*) \rightarrow 0, \quad z^* \rightarrow -\infty, \quad t^* > 0, \tag{23}$$

$$\Delta T_t^*(z^*, 0) = 0, \quad 0 \leq z^* < \infty, \quad t^* = 0, \tag{24}$$

$$\Delta T_s^*(z^*, 0) = 0, \quad -1 \leq z^* \leq 0, \quad t^* = 0, \tag{25}$$

$$\Delta T_f^*(z^*, 0) = 0, \quad -\infty < z^* \leq -1, \quad t^* = 0, \tag{26}$$

The sensitivity problem of Eqs. (15)–(26) can be solved by the same method as the direct problem of Eqs. (1)–(12).

2.4. Adjoint problem and gradient equation

To formulate the adjoint problem, Eqs. (1)–(3) are multiplied by the Lagrange multipliers (or adjoint functions)  $\lambda_t^*$ ,  $\lambda_s^*$ , and  $\lambda_f^*$ , respectively, and the resulting expressions are integrated over the time and correspondent space domains. Then the results are added to the right hand side of Eq. (14) to yield the following expression for the functional  $J[q^*(t^*)]$ :

$$\begin{aligned} J[q^*(t^*)] = & \int_{t^*=0}^{t_f^*} \int_{z^*=-1}^0 [T_s^*(z^*, t^*) - Y^*(z^*, t^*)]^2 \cdot \delta(z^* - z_m^*) dz^* dt^* + \int_{t^*=0}^{t_f^*} \int_{z^*=0}^{\infty} \lambda_t^*(z^*, t^*) \cdot \left[ \frac{\partial^2 T_t^*}{\partial z^{*2}} - \frac{\partial T_t^*}{\partial t^*} \right] dz^* dt^* \\ & + \int_{t^*=0}^{t_f^*} \int_{z^*=-1}^0 \lambda_s^*(z^*, t^*) \cdot \left[ \frac{\partial^2 T_s^*}{\partial z^{*2}} - \frac{\partial T_s^*}{\partial t^*} \right] dz^* dt^* + \int_{t^*=0}^{t_f^*} \int_{z^*=-\infty}^{-1} \lambda_f^*(z^*, t^*) \cdot \left[ \frac{\partial^2 T_f^*}{\partial z^{*2}} - \frac{\partial T_f^*}{\partial t^*} \right] dz^* dt^*. \end{aligned} \tag{27}$$

The variation  $\Delta J$  is derived after  $q^*(t^*)$  is perturbed by  $\Delta q^*(t^*)$ ,  $\lambda_t^*$ ,  $\lambda_s^*$ , and  $\lambda_f^*$  are perturbed by  $\lambda_t^* + \Delta \lambda_t^*$ ,  $\lambda_s^* + \Delta \lambda_s^*$ , and  $\lambda_f^* + \Delta \lambda_f^*$ , respectively, in Eq. (27). Subtracting from the resulting expression the original Eq. (27) and neglecting the second-order terms, we thus find:

$$\begin{aligned} \Delta J[q^*(t^*)] = & \int_{t^*=0}^{t_f^*} \int_{z^*=-1}^0 2[T_s^*(z^*, t^*) - Y^*(z^*, t^*)] \cdot \Delta T_s^* \cdot \delta(z^* - z_m^*) dz^* dt^* + \int_{t^*=0}^{t_f^*} \int_{z^*=0}^{\infty} \lambda_t^*(z^*, t^*) \cdot \left[ \frac{\partial^2 \Delta T_t^*}{\partial z^{*2}} - \frac{\partial \Delta T_t^*}{\partial t^*} \right] dz^* dt^* \\ & + \int_{t^*=0}^{t_f^*} \int_{z^*=-1}^0 \lambda_s^*(z^*, t^*) \cdot \left[ \frac{\partial^2 \Delta T_s^*}{\partial z^{*2}} - \frac{\partial \Delta T_s^*}{\partial t^*} \right] dz^* dt^* + \int_{t^*=0}^{t_f^*} \int_{z^*=-\infty}^{-1} \lambda_f^*(z^*, t^*) \cdot \left[ \frac{\partial^2 \Delta T_f^*}{\partial z^{*2}} - \frac{\partial \Delta T_f^*}{\partial t^*} \right] dz^* dt^*, \end{aligned} \tag{28}$$

where  $\delta(\cdot)$  is the Dirac function. We can integrate the second to the forth double integral terms in Eq. (28) by parts, utilizing the initial and boundary conditions of the sensitivity problem. Then  $\Delta J$  is allowed to go to zero. The vanishing of the integrands containing  $\Delta T_t^*$ ,  $\Delta T_s^*$ , and  $\Delta T_f^*$  leads to the following adjoint problem for the determination of  $\lambda_t^*$ ,  $\lambda_s^*$ , and  $\lambda_f^*$ :

$$\frac{\partial^2 \lambda_t^*(z^*, t^*)}{\partial z^{*2}} + \frac{1}{\alpha_{ts}} \frac{\partial \lambda_t^*(z^*, t^*)}{\partial t^*} = 0, \quad 0 \leq z^* < \infty, \quad t^* > 0, \tag{29}$$

$$\frac{\partial^2 \lambda_s^*(z^*, t^*)}{\partial z^{*2}} + \frac{\partial \lambda_s^*(z^*, t^*)}{\partial t^*} + 2[T_s^*(z_m^*, t^*) - Y^*(z_m^*, t^*)] \delta(z^* - z_m^*) = 0, \quad -1 \leq z^* \leq 0, \quad t^* > 0, \tag{30}$$

$$\frac{\partial^2 \lambda_f^*(z^*, t^*)}{\partial z^{*2}} + \frac{1}{\alpha_{fs}} \frac{\partial \lambda_f^*(z^*, t^*)}{\partial t^*} = 0, \quad -\infty < z^* \leq -1, \quad t^* > 0, \tag{31}$$

$$k_{ts} \lambda_s^*(0, t^*) = \lambda_t^*(0, t^*), \quad z^* = 0, \quad t^* > 0, \tag{32}$$

$$\frac{\partial \lambda_s^*(0, t^*)}{\partial z^*} = \frac{\partial \lambda_t^*(0, t^*)}{\partial z^*}, \quad z^* = 0, \quad t^* > 0, \tag{33}$$

$$k_{fs} \lambda_s^*(-1, t^*) = \lambda_f^*(-1, t^*), \quad z^* = -1, \quad t^* > 0, \tag{34}$$

$$\frac{\partial \lambda_s^*(-1, t^*)}{\partial z^*} = \frac{\partial \lambda_f^*(-1, t^*)}{\partial z^*}, \quad z^* = -1, \quad t^* > 0, \tag{35}$$

$$\lambda_t^*(z^*, t^*) \rightarrow 0, \quad z^* \rightarrow \infty, \quad t^* > 0, \tag{36}$$

$$\lambda_f^*(z^*, t^*) \rightarrow 0, \quad z^* \rightarrow -\infty, \quad t^* > 0, \tag{37}$$

$$\lambda_t^*(z^*, 0) = 0, \quad 0 \leq z^* < \infty, \quad t^* = t_f^*, \tag{38}$$

$$\lambda_s^*(z^*, 0) = 0, \quad -1 \leq z^* \leq 0, \quad t^* = t_f^*, \tag{39}$$

$$\lambda_f^*(z^*, 0) = 0, \quad -\infty < z^* \leq -1, \quad t^* = t_f^*. \tag{40}$$

The adjoint problem is different from the standard initial value problem in that the final time condition at time  $t^* = t_f^*$  is specified instead of the customary initial condition at time  $t^* = 0$ . However, this problem can be transformed to an initial value problem by the transformation of the time variable as  $\tau^* = t_f^* - t^*$ . Then the adjoint problem can be solved by the same method as the direct problem.

Finally the following integral term is left:

$$\Delta J = \int_{t^*=0}^{t_f^*} \lambda_s^*(0, t^*) \Delta q^*(t^*) dt^*. \tag{41}$$

From the definition used in Ref. [10], we have:

$$\Delta J = \int_{t^*=0}^{t_f^*} J'(t^*) \Delta q^*(t^*) dt^*, \tag{42}$$

where  $J'(t^*)$  is the gradient of the functional  $J(q^*)$ . A comparison of Eqs. (41) and (42) leads to the following form:

$$J'(t^*) = \lambda_s^*(0, t^*). \tag{43}$$

### 2.5. Conjugate gradient method for minimization

The following iteration process based on the conjugate gradient method is now used for the estimation of  $q^*(t^*)$  by minimizing the above functional  $J[q^*(t^*)]$ :

$$q^{*K+1}(t^*) = q^{*K}(t^*) - \beta^K p^{*K}(t^*), \quad K = 0, 1, 2, \dots, \tag{44}$$

where  $\beta^K$  is the search step size in going from iteration  $K$  to iteration  $K + 1$ , and  $p^{*K}(t^*)$  is the direction of descent (i.e., search direction) given by:

$$p^{*K}(t^*) = J'^K(t^*) + \gamma^K p^{*K-1}(t^*), \tag{45}$$

which is conjugation of the gradient direction  $J'^K(t^*)$  at iteration  $K$  and the direction of descent  $p^{*K-1}(t^*)$  at iteration  $K - 1$ . The conjugate coefficient  $\gamma^K$  is determined from:

$$\gamma^K = \frac{\int_{t^*=0}^{t_f^*} [J'^K(t^*)]^2 dt^*}{\int_{t^*=0}^{t_f^*} [J'^{K-1}(t^*)]^2 dt^*}, \quad \text{with } \gamma^0 = 0. \tag{46}$$

The convergence of the above iterative procedure in minimizing the functional  $J$  is proved in Ref. [10]. To perform the iterations according to Eq. (44), we need to compute the step size  $\beta^K$  and the gradient of the functional  $J'^K(t^*)$ .

The functional  $J[q^{*K+1}(t^*)]$  for iteration  $K + 1$  is obtained by rewriting Eq. (14) as:

$$J[q^{*K+1}(t^*)] = \int_{t^*=0}^{t_f^*} [T_s^*(q^{*K} - \beta^K p^{*K}) - Y^*(z_m^*, t^*)]^2 dt^*, \tag{47}$$

where we replace  $q^{*K+1}$  by the expression given by Eq. (44). If temperature  $T_s^*(q^{*K} - \beta^K p^{*K})$  is linearized by a Taylor expansion, Eq. (47) takes the form:

$$J[q^{*K+1}(t^*)] = \int_{t^*=0}^{t_f^*} [T_s^*(q^{*K}) - \beta^K \Delta T_s^*(p^{*K}) - Y^*(z_m^*, t^*)]^2 dt^*, \tag{48}$$

where  $T_s^*(q^{*K})$  is the solution of the direct problem at  $z^* = z_m^*$  by using estimated  $q^{*K}(t^*)$  for exact  $q^*(t^*)$  at time  $t^*$ . The sensitivity function  $\Delta T_s^*(p^{*K})$  are taken as the solution of Eqs. (15)–(26) at the measured position  $z^* = z_m^*$  by letting  $\Delta q^* = p^{*K}$  [10]. The search step size  $\beta^K$  is determined by minimizing the functional given by Eq. (48) with respect to  $\beta^K$ . The following expression can be obtained:

$$\beta^K = \frac{\int_{t^*=0}^{t_f^*} \Delta T_s^*(p^{*K}) [T_s^*(q^{*K}) - Y^*] dt^*}{\int_{t^*=0}^{t_f^*} [\Delta T_s^*(p^{*K})]^2 dt^*}. \tag{49}$$

### 2.6. Stopping criterion

If the problem contains no measurement errors, the traditional check condition specified as

$$J(q^{*K+1}) < \eta, \tag{50}$$

where  $\eta$  is a small specified number, can be used as the stopping criterion. However, the observed temperature data contains measurement errors; as a result, the inverse solution will tend to approach the perturbed input data, and the solution will exhibit oscillatory behavior as the number of iteration is increased [29]. Computational experience has shown that it is advisable to use the discrepancy principle [28] for terminating the iteration process in the conjugate gradient method. Assuming  $T_s^*(z_m^*, t^*) - Y^*(z_m^*, t^*) \cong \sigma$ , the stopping criteria  $\eta$  by the discrepancy principle can be obtained from Eq. (14) as

$$\eta = \sigma^2 t_f^*, \tag{51}$$

where  $\sigma$  is the standard deviation of the measurement error. Then the stopping criterion is given by Eq. (50) with  $\eta$  determined from Eq. (51).

### 2.7. Computational procedure

The computational procedure for the solution of this inverse problem may be summarized as follows:

Suppose  $q^{*K}(t^*)$  is available at iteration  $K$ .

- Step 1. Solve the direct problem given by Eqs. (1)–(12) for  $T_t^*(z^*, t^*)$ ,  $T_s^*(z^*, t^*)$ , and  $T_f^*(z^*, t^*)$ , respectively.
- Step 2. Examine the stopping criterion given by Eq. (50) with  $\eta$  given by Eq. (51). Continue if not satisfied.
- Step 3. Solve the adjoint problem given by Eqs. (29)–(40) for  $\lambda_t^*(z^*, t^*)$ ,  $\lambda_s^*(z^*, t^*)$ , and  $\lambda_f^*(z^*, t^*)$ , respectively.
- Step 4. Compute the gradient of the functional  $J'(t^*)$  from Eq. (43).
- Step 5. Compute the conjugate coefficient  $\gamma^K$  and direction of decent  $p^{*K}(t^*)$  from Eqs. (46) and (45), respectively.
- Step 6. Set  $\Delta q^*(t^*) = p^{*K}(t^*)$  and solve the sensitivity problem given by Eqs. (15)–(26) for  $\Delta T_t^*(z^*, t^*)$ ,  $\Delta T_s^*(z^*, t^*)$ , and  $\Delta T_f^*(z^*, t^*)$ , respectively.
- Step 7. Compute the search step size  $\beta^K$  from Eq. (49).
- Step 8. Compute the new estimation for  $q^{*K+1}(t^*)$  from Eq. (44) and return to Step 1.

## 3. Results and discussion

The objective of this article is to validate the present approach when used in estimating the unknown time-dependent frictional heat generation at the interface of two semi-spaces during a sliding contact accurately with no prior information



on the functional form of the unknown quantities, a procedure called function estimation. In order to illustrate the importance of the relative position between the measured quantity (temperature  $Y^*$ ) and the estimated quantity (heat generation  $q^*$ ) on the solution accuracy, we first consider the simulated exact value of  $q^*(t^*)$  as a simple sinusoidal variation over the time period  $t^* = 0-1$ :

$$q^*(t^*) = 100 \sin(t^*\pi). \tag{52}$$

In the present study, we assume the materials of the two semi-spaces being identical and made of steel ( $k_t = k_f = 42 \text{ W m}^{-1} \text{ K}^{-1}$  and  $\alpha_t = \alpha_f = 1.2 \times 10^{-5} \text{ m}^2 \text{ s}^{-1}$ ), while the material of the strip is aluminum ( $k_s = 209 \text{ W m}^{-1} \text{ K}^{-1}$  and  $\alpha_s = 8.6 \times 10^{-5} \text{ m}^2 \text{ s}^{-1}$ ). The thickness of the strip  $d$  is taken as  $300 \mu\text{m}$  [7].

The numerical procedure in this paper is based on the unstructured-mesh, fully collocated, finite-volume code, 'US-TREAM' developed by the first named author. This is the descendent of the structured-mesh, multi-block code of 'STREAM' [30]. Since the sliding-contact interface ( $z^* = 0$ ) is the most important part in this problem, fine meshes are used on either sides of the interface and the strip, where there are 50 cells in this layer. For the rest of the domain, coarser meshes are applied. Both semi-spaces also extend a length of 20 outwards from either sides of the sliding-contact interface, and there are 80 cells allocated for each semi-space with most of the cells being concentrated towards the sliding surface. In total, there are 210 cells for the entire computational domain. This mesh has been proved in a grid-independent test to achieve grid-independent solutions. A single thermocouple is assumed to be located at three different positions,  $z_m^* = 0.0, -0.5,$  and  $-0.7,$  respectively, in the coating layer to test the sensitivity of solution accuracy on the relative position between the measured and estimated quantities. In terms of the time domain, the total dimensionless measurement time is chosen as  $t_f^* = 1.0$  and measurement time step is set as 0.01.

In the analysis, we do not have a real experimental set up to measure the temperature  $Y^*(z_m^*, t^*)$  in Eq. (14). Instead, we assume a real heat generation,  $q^*(t^*)$  of Eq. (52), and substitute the exact  $q^*(t^*)$  into the direct problem of Eqs. (1)–(12) to calculate the temperatures at the location where the thermocouple is placed. The results are taken as the computed temperature  $Y_{exact}^*(z_m^*, t^*)$ . Nevertheless, in reality, the temperature measurements always contain some degree of error, whose magnitude depends upon the particular measuring method employed. In order to take measurement errors into account, a random error noise is added to the above computed temperature  $Y_{exact}^*(z_m^*, t^*)$  to obtain the measured temperature  $Y^*(z_m^*, t^*)$ . Hence, the measured temperature is expressed as:

$$Y^*(z_m^*, t^*) = Y_{exact}^*(z_m^*, t^*) + \varpi\sigma, \tag{53}$$

where  $\varpi$  is a random variable within  $-2.576$  to  $2.576$  for a 99% confidence bounds, and  $\sigma$  is the standard deviation of the measurement. The measured temperature  $Y^*(z_m^*, t^*)$  generated in such way is termed simulated measurement temperature.

Fig. 2 shows the estimated values of the unknown function  $q^*(t^*)$ , obtained with the initial guesses  $q^{*0} = 0$ , measurement error of deviation  $\sigma = 0.0$ , and  $z_m^* = 0.0, -0.5,$  and  $-0.7,$  termed case 1, 2, and 3, respectively. These results show that the estimated quantity is in very good agreement with that of the exact values only in case 1, where the measured and estimated quantities are at the same position. However, the predictive accuracy deteriorates when the measurement position moves away from the estimated position as can be seen in cases 2 and 3. Moving the measurement position further beyond  $z_m^* = -0.7$  results in instability, and the inverse iteration does not converge. The results clearly show a certain degree of sen-

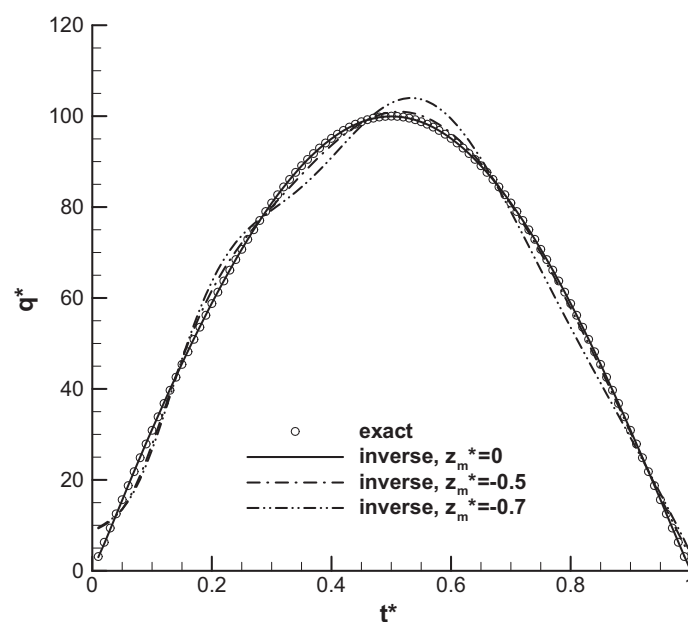


Fig. 2. Estimated  $q(t^*)$  with the initial guesses  $q^{*0} = 0.0$ , measurement error  $\sigma = 0.0$ , and measurement location  $z_m^* = 0.0, -0.5,$  and  $-0.7.$

sitivity of the predictive accuracy on the relative position between the measured and the estimated quantities, a phenomenon that has been repeatedly reported by a number of studies mentioned in Section 1. However, the causes contributing to the sensitivity have not yet been well documented. The comparison between the exact and the inversed temperatures at the measurement positions is given in Fig. 3. Despite the discrepancies between the exact and the inverse values observed in cases 2 and 3, the inverse temperature at all measurement positions show almost perfect agreement with the measurement temperature, an indication that the inverse iterations in all three cases have actually converged. Therefore, the discrepancies in Fig. 2 for cases 2 and 3 are not contributed by the instability of the inverse iteration procedure. To find out where the discrepancies are rooted in, we need to understand the functional relation between the measured quantity and the estimated quantity. Fig. 4(a) shows the exact temperature distributions versus time at the three measurement positions over the period of  $t^* = 0-0.1$  with the  $q^*(t^*)$  of Eq. (52). In the current transient heat conduction problem, any disturbance at one point in space needs certain time to ripple outwards to reach other places; and this has been shown clearly in Fig. 4(a). Here, only the temperature at  $z_m^* = 0$  has immediate respond to the onset of heat generation. The temperatures at the other two positions, on the other hand, start to develop only after  $t^* = 0.02$  or  $0.03$ . This demonstrates that at the first few time steps, the measurement temperatures for cases 2 and 3, especially the latter where the measurement position is located further away from the heat generation position, are almost independent of the heat generation located at  $z^* = 0$ . The temperature distributions versus time at  $z_m^* = -0.7$  from another test by respectively setting constant  $q^*(t^*) = 5, 50, \text{ and } 100$  are plotted in Fig. 4(b). Despite the variations in the value of  $q^*(t^*)$ , the temperature at  $z_m^* = -0.7$  remains almost zero before  $t^* = 0.03$ , a further definite proof that the two quantities are indeed independent during a brief initial time period. To understand how this functional independency affects the inverse algorithm, we first need to know how the mechanism to correct the estimated quantity works in the current inverse procedure.

Eq. (30) implies that the magnitude of  $\lambda_s^*$  over the domain is mainly generated by the source term  $2[T_s^*(z_m^*, t^*) - Y^*(z_m^*, t^*)]$  at the measurement location; in other words,  $\lambda_s^*$  is fed by the disagreement between the computed and measured temperatures at the measurement location. Then the amount of the disagreement is used to correct  $q^*(t^*)$  via Eq. (44). In a sense, the measured and the estimated quantities need to communicate with each other in every time step for the correction mechanism to perform well. If there is no distance between the two quantities, the communication is immediate, and the correction is effective. On the other hand, if the two quantities are parted by some distance, there will be a time lag for them to communicate. The impact of this lag in communication on the solution accuracy will be discussed later. Another important factor affecting the correction mechanism is the marching of time in the adjoint problem. Comparing Eqs. (2) with (30), the governing equations of the direct and the adjoint problems in the coating layer, it can be noted that their time-dependent terms are at different sign. This suggests that from the aspect of  $\lambda_s^*$ , the time is marching backwards. Indeed, the initial condition of the adjoint problem is at  $t^* = t_f^*$  as stated in Eq. (38). This is the final important factor affecting the inverse correction mechanism, and now we can weave the relation of solution accuracy with the independency between the measured and estimated quantities, the source term in the adjoint problem, the time lag in communication, and the backward time marching in the adjoint problem as follows: For case 3, the independency between the measured and estimated quantities before  $t^* \leq 0.03$  results in a zero source term  $[T_s^*(z_m^*, t^*) - Y^*(z_m^*, t^*)]$  in the adjoint problem's governing equation. However, from the aspect of the adjoint problem, this disappearance of source term actually occurs at the last few time steps because of the

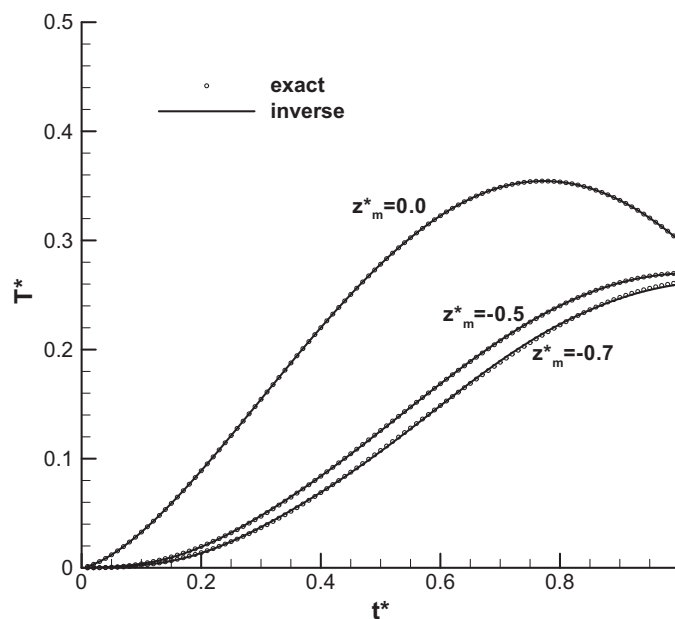
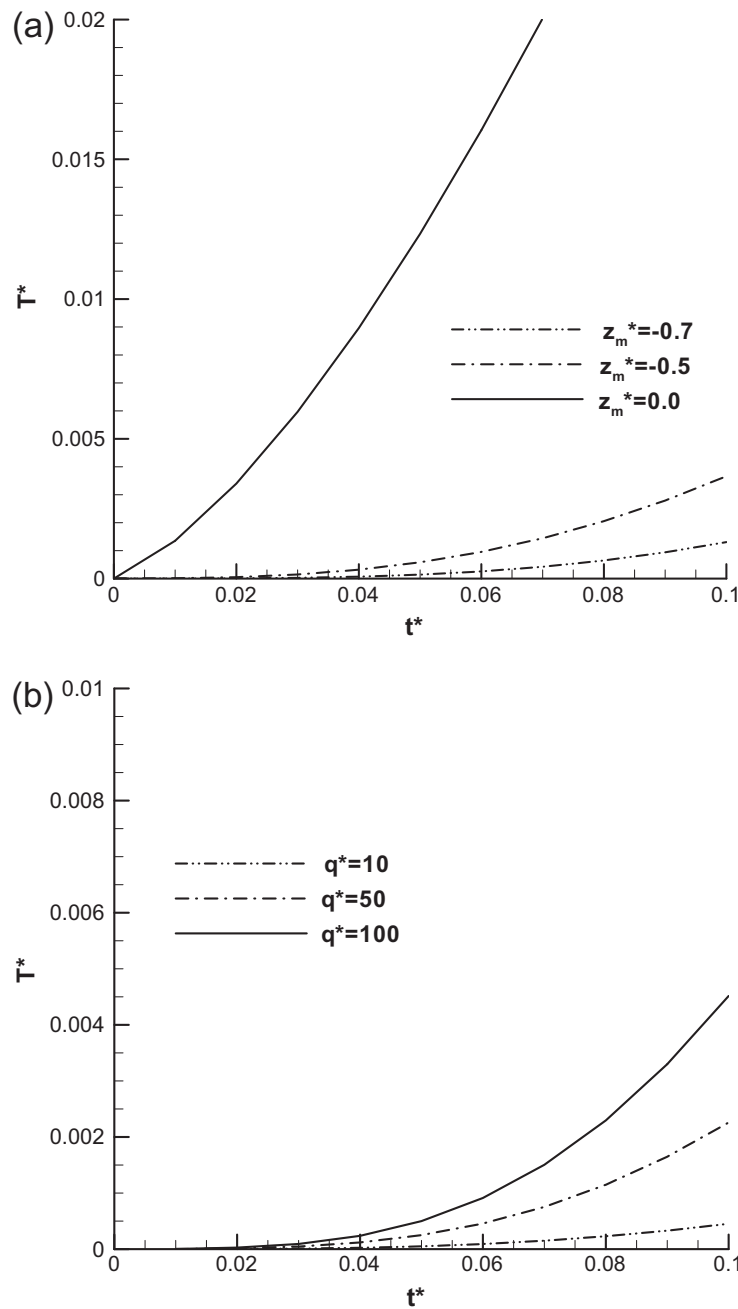


Fig. 3. Temperature distributions at the measurement positions with initial guesses  $q^{*0} = 0.0$ , measurement error  $\sigma = 0.0$ , and measurement positions  $z_m^* = 0.0, -0.5, \text{ and } -0.7$ .



**Fig. 4.** Temperature distributions at the initial time steps; (a) at locations  $z_m^* = 0.0, -0.5$ , and  $-0.7$ , and (b) at  $z_m^* = -0.7$  but with  $q^*(t^*) = 5, 50, 100$ .

backward time marching. The disappearance of source term also means that there is no communication between the measured and estimated quantities; hence the correction mechanism does not work during these few time steps. Although the communication stops during this brief period of time, some false information still goes through, due to the communication time lag, and results in inaccurate  $q^*(t^*)$  for the first few time steps at the end of the inverse iteration. This can be explained as: at the early stage of the inverse iteration, the difference between the measured and estimated quantities is very large; hence the source term in the adjoint problem is also very large for each time step, thus giving rise to a generally high level of  $\lambda_s^*$  which then ripples outwards in space as time marches. When it reaches the position of the estimated quantity, via the backward time marching, it can be picked up by Eq. (44) to correct  $q^*(t^*)$ . Therefore, this initial high level of  $\lambda_s^*$  can be regarded as ‘false information’ that affects the accuracy of the correction mechanism. In case 1, the false information will gradually die out as the source term diminishes when the inverse iteration is converging, thus it does not affect the final result. Nevertheless, in case 3, the false information has been picked up by Eq. (44) and given rise to some incorrect  $q^*(t^*)$  at the early stage of the inverse iteration, the wrongly created  $q^*(t^*)$  for the first few time steps will remain there through the entire inverse iteration because in the corresponding time steps of the adjoint problem, the source term is always zero no matter the value of  $q^*(t^*)$  is. That is, the only information that has been used to correct  $q^*(t^*)$  for the first few time steps is actually

the false information created in the initial inverse iteration stage. A proof of this can be seen in Fig. 2 where the inverse  $q^*(t^*)$  in cases 2 and 3 is a bit higher than the exact value at the initial few time steps. As the heat generation magnitude has been wrongly estimated initially, the subsequent estimation of  $q^*(t^*)$  cannot be accurate because the inverse algorithm has to create an incorrect  $q^*(t^*)$ -profile to compensate the historical effect left by the initial wrongly predicted  $q^*(t^*)$ .

After the effect of the relative position between the measured and estimated quantities on the solution accuracy been well discussed, attention can now be directed towards the solving of the current inverse problem with the measured and estimated quantities being at the same position. The estimated temperature distributions in case 1 for  $t^* = 0.1, 0.5$ , and  $0.9$ , respectively, are shown in Fig. 5. These results confirm that the estimated temperature values are in very good agreement with those of the exact values for the case considered in this study if the measured and the estimated quantities are at the same position. It can be found in Fig. 5 that overall, the temperature increases as time elapses. In addition, the temperature rises rapidly at the interface due to the rapid rise of the heat generation, but it drops sharply towards the ambient temperature as the distance from the interface increases. Fig. 6 illustrates the inverse solutions of  $q(t^*)$ , obtained with the initial guess values  $q^{*0} = 0.0$ , measurement error of deviation  $\sigma = 0.01$ , and temperature measurement taken at  $z_m^* = 0$ . For a

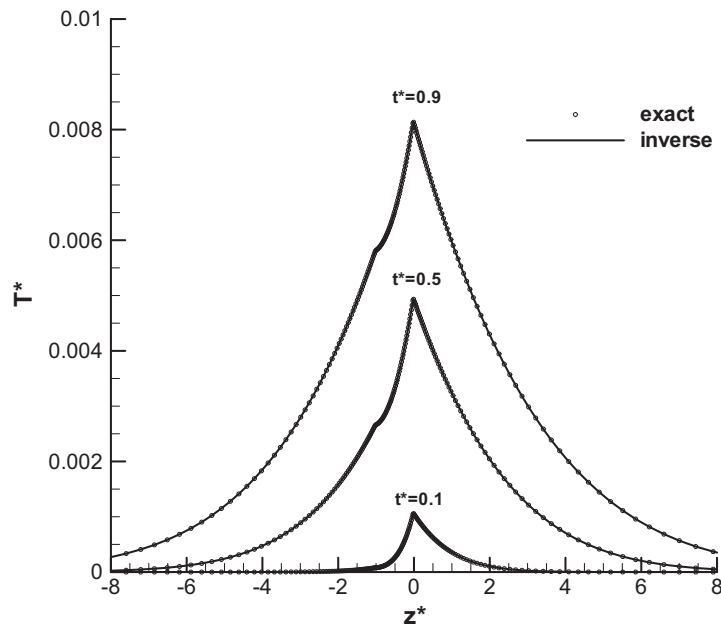


Fig. 5. The overall temperature distributions for  $t^* = 0.1, 0.5$ , and  $0.9$ , respectively.

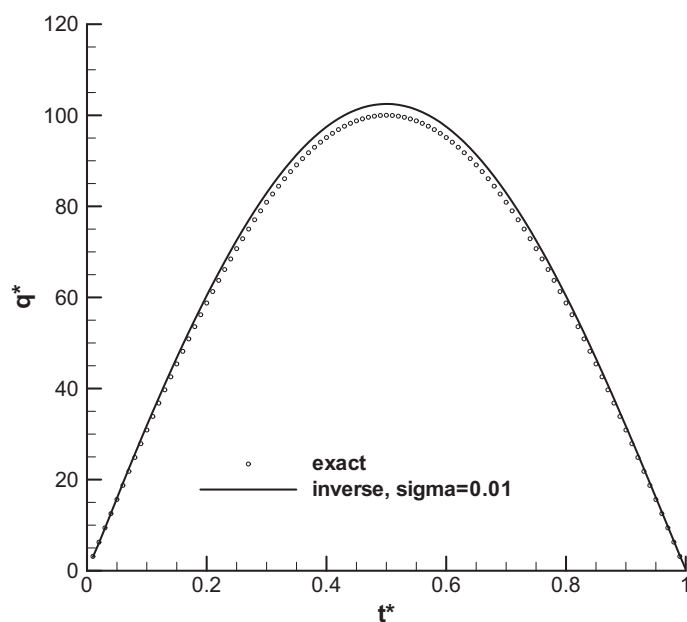


Fig. 6. Estimated  $q(t^*)$  with the initial guesses  $q^{*0} = 0.0$ , measurement error  $\sigma = 0.01$ , and measurement location  $z_m^* = 0.0$ .

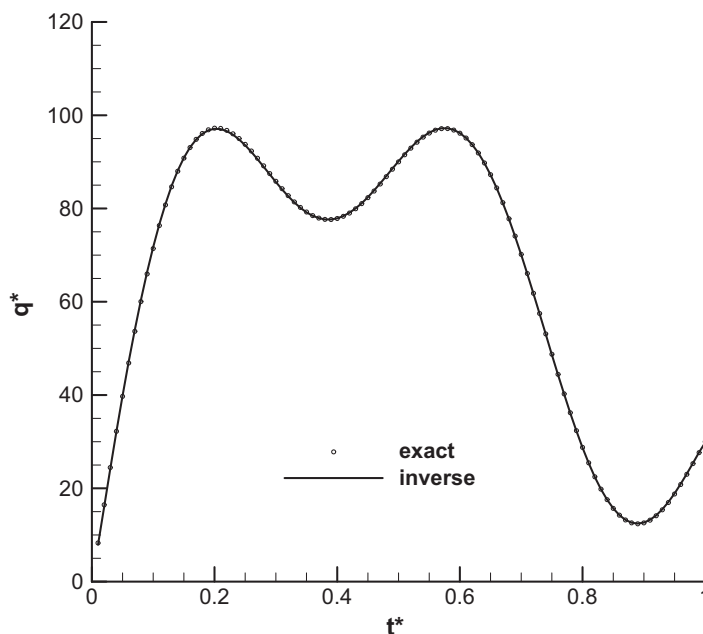


Fig. 7. Estimated  $q^*(t^*)$  of Eq. (53) with the initial guesses  $q^{*0} = 0.0$ , measurement error  $\sigma = 0.0$ , and measurement location  $z_m^* = 0.0$ .

temperature of unity and 99% confidence, that standard deviation,  $\sigma = 0.01$ , corresponds to measurement error of 2.58%. Fig. 6 reveals that the maximum error due to this measurement error is about 2.4%. This shows that for the cases considered in this study, an increase in the measurement error does not cause obvious deterioration on the accuracy of the inverse solution.

In order to demonstrate the capability of the presented methodology in obtaining an accurate estimation no matter how complex the unknown function is, we consider another case of exact  $q^*(t^*)$  with the following form:

$$q^*(t^*) = 100 \cdot [0.3 \times \sin(2\pi t^*) + 0.25 \times \sin(4\pi t^*) + 3t^* \times (1.1 - t^*)]. \quad (54)$$

Fig. 7 shows the estimated  $q^*(t^*)$ , obtained with the initial guesses  $q^{*0} = 0$  and measurement error of deviation  $\sigma = 0.0$ . It is noticeable in Fig. 7 that an excellent estimation still can be obtained with this complex unknown function.

#### 4. Conclusion

An inverse algorithm based on the conjugate gradient method and the discrepancy principle was successfully applied to the inverse problem to determine the unknown time-dependent frictional heat generation at the interface of two semi-spaces during a sliding contact, while knowing the temperature history at some measurement locations. The results show that the relative position between the measured and the estimated quantities dictates the accuracy of the inverse method. Highly accurate estimation can be achieved when the position of the measured quantity is very close to that of the estimated quantity. The accuracy, however, deteriorates as the positions of the two quantities are parted by some distance; and the causes behind this have been well discussed.

If the measured and the estimated quantities are at the same position, the numerical results confirm that the method can accurately estimate the time-dependent heat generation and temperature distributions for the problem even involving the inevitable measurement errors. The proposed inverse algorithm does not require prior information for the functional form of the unknown quantities to perform the inverse calculation, and excellent estimated values can be obtained for the considered problem. The methodology of the present study can be applied to the prediction of heat generation in a wide range of engineering problems involving sliding-contact elements.

#### Acknowledgements

This work was supported by the National Science Council, Taiwan, Republic of China, under the Grant Nos. NSC 97-2221-E-168-041 and NSC 97-2221-E-168-039. The authors are also grateful for the help from Mrs. Shin-Liang Chen in FooYin University.

#### References

- [1] A.A. Yevtushenko, E.G. Ivanyk, O.V. Sykora, The transitive temperature processes in local friction contact, *Int. J. Heat Mass Transfer* 38 (1995) 2395–2401.

- [2] A.A. Yevtushenko, E.G. Ivanyk, O.O. Yevtushenko, Exact formulae for determination of the mean temperature and wear during braking, *Heat Mass Transfer* 35 (1999) 163–169.
- [3] A. Evtushenko, M. Kutsei, Non-stationary frictional heat problem for plane-parallel half-space system, *J. Friction Wear* 28 (2007) 246–259.
- [4] A.A. Yevtushenko, M. Kuciej, Influence of convective cooling on the temperature in a frictionally heated strip and foundation, *Int. Commun. Heat Mass Transfer* 36 (2009) 129–136.
- [5] A. Evtushenko, S. Matysiak, M. Kutsei, Thermal problem of friction at braking of coated body, *J. Friction Wear* 26 (2004) 33–40.
- [6] A.A. Yevtushenko, M. Rozniakowska, M. Kuciej, Transient temperature processes in composite strip and homogeneous foundation, *Int. Commun. Heat Mass Transfer* 34 (2007) 1108–1118.
- [7] A.A. Yevtushenko, M. Kuciej, Influence of the protective strip properties on distribution of the temperature at transient frictional heating, *Int. J. Heat Mass Transfer* 52 (2009) 376–384.
- [8] S. Lorenzode, M. Loddo, Effect of frictional heating thermal advection on pre-seismic sliding: a numerical simulation using a rate-, state-, and temperature-dependent friction law, *J. Geodyn.* 49 (2010) 1–13.
- [9] R.M. Hestenes, E. Stiefel, Methods of conjugate gradients for solving linear systems, *J. Res. Natl. Bur. Stand.* 49 (1952) 409–436.
- [10] O.M. Alifanov, *Inverse Heat Transfer Problem*, Springer-Verlag, 1994, pp. 172–178.
- [11] Y.C. Yang, H.L. Lee, W.J. Chang, An inverse problem in simultaneously estimating boundary moisture fluxes in a porous annular cylinder, *Acta Mech.* 179 (2005) 131–144.
- [12] Y.C. Yang, Simultaneously estimating the contact heat and mass transfer coefficients in a double-layer hollow cylinder with interface resistance, *Appl. Therm. Eng.* 27 (2007) 501–508.
- [13] W.L. Chen, Y.C. Yang, On the inverse heat convection problem of the flow over a cascade of rectangular blades, *Int. J. Heat Mass Transfer* 51 (2008) 4184–4194.
- [14] W.L. Chen, Y.C. Yang, Estimation of the transient heat transfer rate at the boundary of an electronic chip packaging, *Numer. Heat Transfer Part A* 54 (2008) 945–961.
- [15] R.S. Banim, M.J. Tierney, P.N. Brett, A nonlinear indirect measurement problem for a multi thermocouple probe immersed in a liquid, *Numer. Heat Transfer Part A* 40 (2001) 103–116.
- [16] N. Al-Khalidy, A general space marching algorithm for the solution of two-dimensional boundary inverse heat conduction problems, *Numer. Heat Transfer Part A* 34 (1998) 339–360.
- [17] C. Niliot Le, F. Lefevre, Multiple transient point heat sources identification in heat diffusion: application to numerical two- and three-dimensional problems, *Numer. Heat Transfer Part B* 39 (2001) 277–301.
- [18] M. Raudensky, K.A. Woodbury, J. Kral, Genetic algorithm in solution of inverse heat conduction problems, *Numer. Heat Transfer Part B* 28 (1995) 293–306.
- [19] A.J. Neto Silva, M.N. Ozisik, Two-dimensional inverse heat conduction problem of estimating the time-varying strength of a line heat source, *J. Appl. Phys.* 71 (1992) 5357–5362.
- [20] C.Y. Yang, Solving the two-dimensional inverse heat source problem through the linear least-squares error method, *Int. J. Heat Mass Transfer* 41 (1998) 393–398.
- [21] C. Niliot Le, F. Lefevre, A parameter estimation approach to solve the inverse problem of point heat sources identification, *Int. J. Heat Mass Transfer* 47 (2004) 827–841.
- [22] B. Jin, L. Marin, The method of fundamental solutions for inverse source problems associated with the steady-state heat conduction, *Int. J. Numer. Methods Eng.* 69 (2007) 1570–1589.
- [23] H.L. Lee, W.J. Chang, W.L. Chen, Y.C. Yang, An inverse problem of estimating the heat source in tapered optical fibers for scanning near-field optical microscopy, *Ultramicroscopy* 107 (2007) 656–662.
- [24] W.L. Chen, Y.C. Yang, S.S. Chu, Estimation of heat generation at the interface of cylindrical bars during friction process, *Appl. Therm. Eng.* 29 (2009) 351–357.
- [25] S.K. Wu, H.S. Chu, Inverse determination of surface temperature in thin-film/substrate systems with interface thermal resistance, *Int. J. Heat Mass Transfer* 47 (2004) 3507–3515.
- [26] C.K. Chen, L.W. Wu, Y.Z. Yang, Estimation of time-varying inlet temperature and heat flux in turbulent circular pipe flow, *J. Heat Transfer* 128 (2006) 44–52.
- [27] J. Su, A.T. Chwang, Estimation of heat transfer coefficient of cryogen spray cooling with Alifanov's iterative regularization method, *Numer. Heat Transfer Part A* 51 (2007) 781–794.
- [28] O.M. Alifanov, E.A. Artyukhin, Regularized numerical solution of nonlinear inverse heat-conduction problem, *J. Eng. Phys.* 29 (1975) 934–938.
- [29] O.M. Alifanov, Application of the regularization principle to the formulation of approximate solution of inverse heat conduction problem, *J. Eng. Phys.* 23 (1972) 1566–1571.
- [30] F.S. Lien, W.L. Chen, M.A. Leschziner, A multiblock implementation of a non-orthogonal, collocated finite volume algorithm for complex turbulent flows, *Int. J. Numer. Methods Fluids* 23 (1996) 567–588.